Parametric modelling of magnetic fine particle systems: the role of single domain particle size distributions and magnetic anisotropy

2005 J. Phys.: Conf. Ser. 17 1

(http://iopscience.iop.org/1742-6596/17/1/001)

Institute of Physics Publishing Journal of Physics: Conference Series **17** (2005) 1–6
doi:10.1088/1742-6596/17/1/001 Fifth International Conference on Fine Particle Magnetism

Parametric modelling of magnetic fine particle systems: the role of single domain particle size distributions and magnetic anisotropy

S R Hoon and D B Lambrick
Manchester Metropolitan University, Department of Environmental and Geographical Sciences, Manchester, M1 5GD, UK

E-mail: s.hoon@mmu.ac.uk

Abstract. We demonstrate the effects and role of anisotropy and particle size distributions upon the values of constitutive parameters determined from experimental *M(H)* loops of single domain nanoparticle systems. We employ experimental and magnetic material parameters as inputs to a numerical programme run from a graphical user interface (GUI) to permit modelling and interpretation of experimental data and assessment of the stability of the constitutive parameters so derived and characterisation of the departures observed from pure Langevin behaviour.

1. Introduction:

Modelling of the field, H, and temperature, T, dependent variation of magnetisation, $M(H,T)$, and susceptibility, $\kappa(H,T)$, has been used extensively to gain insight into the fundamental magnetic behaviour of fine particle systems. Candidate systems embrace amorphous or thin film nanoparticles, superparamagnetic (SPM) single domain (SD) particles, colloids and magnetic fluids, pseudo-single domain (PSD) geogenic materials, and environmental sediments used in source apportionment, the establishment of temporal or climatic proxies and diagenetic processes. Parametric and constitutive parameters such as initial susceptibility, κ_i, saturation, M_s, and remanent, M_r, magnetisation, coercive, H_c, and remanent coercive, H_r, fields and their ratios (e.g. M_r/M_s) and temperature dependence derived from $M(H,T)$ and $\kappa(H,T)$ are employed in magnetic granulometry to determine particle distribution parameters V and σ [1, 2, 3, 4, 5, 6] in turn used to interpret magnetic behaviour [7, 8]. There is however interdependence in the values of M_s, K, V and σ determined from $M(H,T)$ and $\kappa(H,T)$. Reliability of the latter is important as they are used to gain understanding of magnetic behaviour and effects [9]. The effect of K [10, 11], V and σ upon the behaviour and interpretation of SD and SPM systems has been of interest for some time, studied using graphical techniques [12] or restricted cases [13].

2. Experimental Method

We employ numerical solutions using experimental parameters K, T, H_c, M_s, $\kappa(H)$, V, σ as inputs to a Graphical User Interface (GUI) to model experimental data and assess the stability of derived magnetic parameters and determine the effects of K and size distributions upon the values of constitutive parameters determined from experimental $M(H)$ loops. We consider assemblies of SD particles above their blocking temperature i.e. of zero coercivity. Where the energy of an assembly of SD particles of saturation magnetisation, M_s, volume, V, and moment $m = M_sV$ depends solely upon the applied field, $\mu_0 B$, the magnetisation may be determined analytically from the probability, Π_B, that

a magnetic moment will occupy a thermally populated Zeeman energy state, E_B, determined by the field to thermal energy ratio, $\Pi_B \propto \exp(E_B / kT) = \exp(m \cdot B / kT)$. In the absence of other energy terms integrating over the cylindrically symmetric energy states between the applied field and moment angles yields for a monodispersed system, $M(H)/M_S = f(E_B / kT) = L(x)$ where $L(x)$ is the Langevin function. However, if demagnetisation, E_D, magnetostriction, E_{MS}, or magnetocrystalline, E_C, energies are non zero, departures from ideal Langevin SPM, (LSPM), are expected and the integral defining $M(H)/M_S = f\left(E(\phi,\alpha,\omega,\vartheta,\eta)/kT\right)$ must be evaluated numerically[12], where $E = E_B + E_D + E_{MS} + E_C$, ϕ is the angle between the applied field and particle moment and θ,η and α,ω are the azimuthal and polar angles with respect to H and particle anisotropy axes, $\hat{c}_i$, respectively. Where a SD system possesses a particle size distribution, departures from LSPM behaviour are expected as even in the absence of magnetic anisotropy m is distributed via the volume number distribution as $M_sV \times P(\mu,\sigma)$, [7,8]. Restricted classes of the *Brillouin* function such as the *tanh* function, $T(x)$, are normally only anticipated for monodispersed systems in the presence of dominant negative uniaxial anisotropy and coaxial easy axis alignment. Although our approach is generic we have applied it in particular to colloidal materials and environmental sediments and source apportionment.

3. Results and discussion

The effect of the particle size distribution upon magnetisation curves. We present numerical data for $M(V,\sigma)$ appropriate to Gaussian, P_G, triangular, P_T, rectangular, P_R, and log-normal, P_{LN}, particle volume distributions. Fig.1a contrasts normalised P_G, P_T, and P_R, particle number volume distributions. The parameter $b = m/kT$ where $m = M_sV$. The differences between the P_G and P_T are particularly small. Consequently although $M(H)$ determined by the corresponding moment distributions, $V \times P(V)$, exhibits larger differences, fig.1b, they may be insufficient to generate experimentally discernable differences in $M(H)$, fig. 2. Similar effects are demonstrated for the log-normal distribution, figs 3 and 4. Comparison of fig.4a and fig.4b shows that the difference between P_G and P_{LN} for $L(x)$ and $T(x)$ never exceeds 1%. The moment distribution is very similar for the P_G and

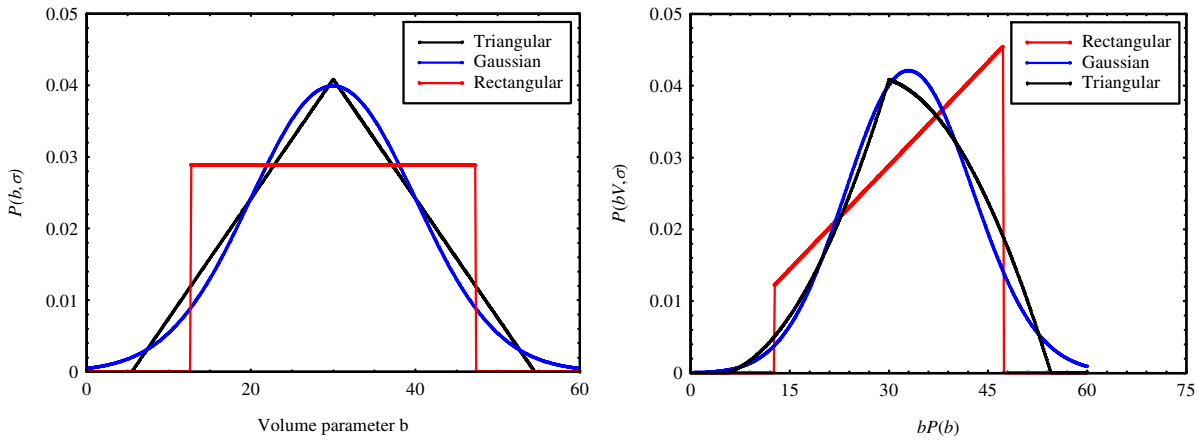

Fig.1a a. Normalised P_T, P_G, and P_R distributions, b=30, σ=10

Fig 1b. P_T, P_G, and P_R moment distributions, b=30, σ=10

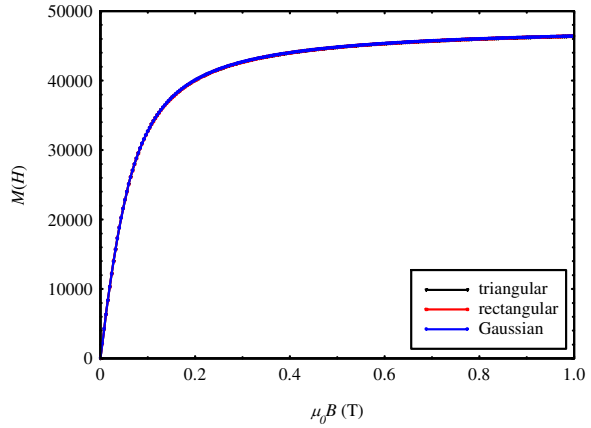

Fig.2a $M(H)$, $L(x)$ convolved with P_T, P_G, and P_R

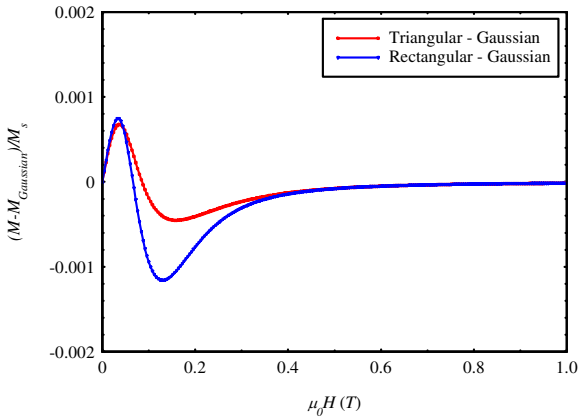

Fig.2b $M(H)$ difference plots for fig.2a

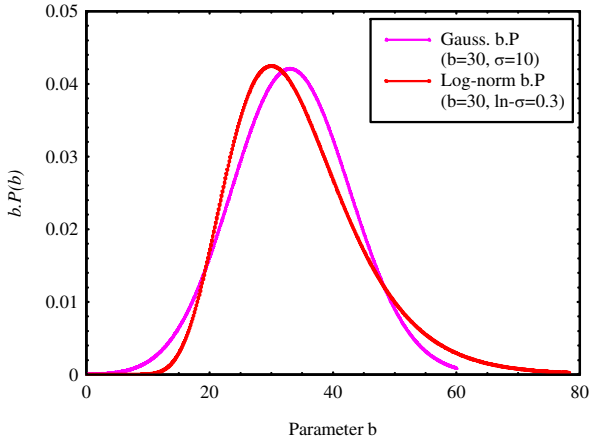

Fig.3 Moment distributions for P_G and P_{LN}, b=30, σ=10

P_{LN} distributions where ln(σ) has been optimised to minimise the difference between the distributions, fig.5. Only σ_{LN} has been varied and is optimum at 0.39 when the $M(H)$ curves overlay to within 0.2% of M_S. As σ increases κ_i increases, κ_h decreases and at high field $M(H)$ converges on the mono dispersed curve, an effect that mimics weak to moderate anisotropy, see later. Figs 2 to 5 inclusive demonstrate the weak sensitivity of $M(H)$ to the functional form of the particle volume distribution consistent with the notion that the derivation of volume distributions from magnetisation curves alone is ill posed. It is more important to acknowledge that a volume distribution exists than to attempt to define its functional from magnetic data alone. The dominant effect is that of the intrinsic magnetisation function, $L(x)$ or $T(x)$ even in the presence of a particle size distribution. Hence the magnetisation functional chosen and loop shape exhibited are determined by intrinsic material processes. We have found that many environmental materials are modelled to high accuracy by either mono-dispersed ferri-*L(x)* plus paramagnetic term, (river bedload sediments), mono-dispersed ferri-*T(x)* plus paramagnetic term (bauxite / coral sediments) and have explored possible reasons for this behaviour.

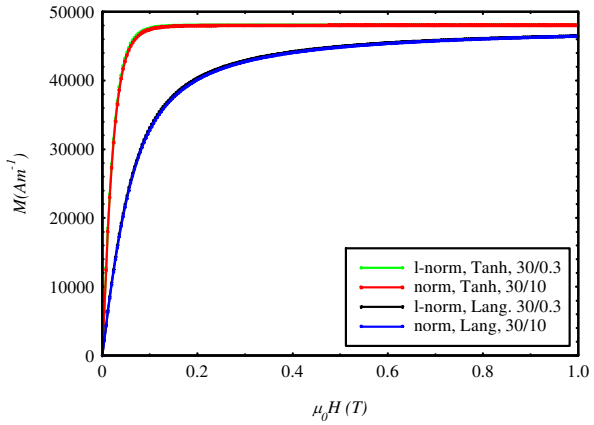

Fig.4a. $M(H, \sigma)$ for P_G and P_{LN} convolved with $L(x)$ and $T(x)$, b=30

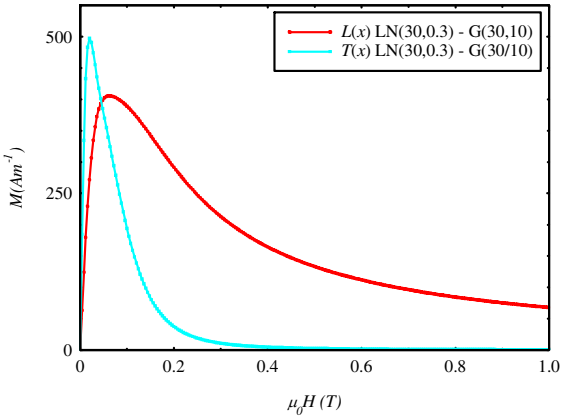

Fig.4b $M(H, \sigma)$ difference plots for fig.4a

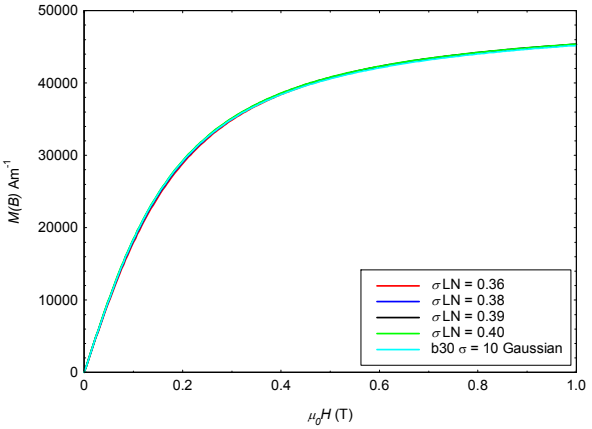

Fig.5a. $M(H, \sigma)$ for P_G and P_{LN} b=30 convolved with $L(x)$ σ=10, σ_{LN}: 0.36, 0.38, 0.39, 0.4

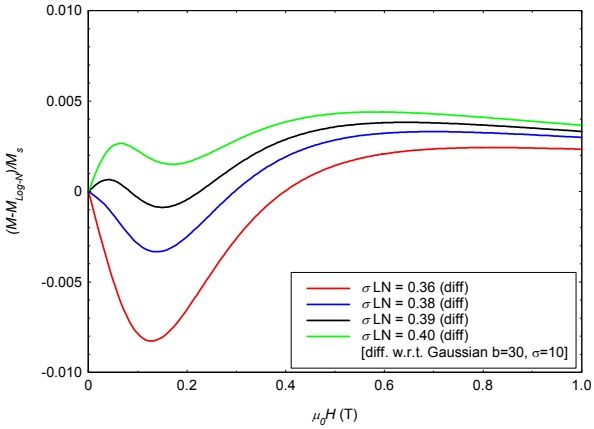

Fig.5b. $M(H, \sigma)$ difference plots for fig.5a

The effect of magnetic anisotropy upon M(H). Fig.6 indicates the effect of uniaxial anisotropy upon the $M(H)$ curve. For monodispersed systems departures from ideal SPM behaviour occur for R as low as 5, where $R = KV/kT$, well within the criterion of R<25 values generally accepted as necessary for observation of SPM behaviour. Such departures from SPM can be confused experimentally with, or obscured by, the existence of a particle volume distribution. Dependent upon R, medium and high field *M(H)* may depart significantly from pure (K=0) Langevin SPM, (LSPM). For $10 < R < 25$ and typical experimental fields and temperature ($5 < \mu_0 bH < 30$) significant departures from LSPM behaviour are observed. It is then possible to confuse the presence of strong uniaxial anisotropy with a binary mixture of SPM and pure (high temperature) paramagnetic components. This is of importance to sediment source apportionment and source unmixing. Whilst the commonly agreed condition of $R <$ 25 is sufficient for the observation of SPM behaviour it is not sufficient for deconvolution of the effects of K and a particle size distribution. The effect of this convolution is most noticeable for negative uniaxial anisotropy, K_u<0, fig.6a, due to both the larger energy barrier to moment rotation and restricted number (two) of easy directions, $\hat{c}$. Fig.6b demonstrates the effect for K_u>0 where easy axes $\hat{c}$ all lie in the basal plane. Consequently the particles possess no energy barrier. For

monodispersed systems the initial susceptibility, κ_i, is independent of K, fig.6a,b. Hence the κ_i is effected by the volume distribution alone. However, as the high field susceptibility, $\kappa_h = dM/dH$ is K dependent, particle distribution parameters determined from fitting techniques that use κ_i and κ_h, [6] and asymptotic linear approach of $M(1/H)$ to saturation εM_s as $1/H \rightarrow 0$, are prone to over estimate the contribution of small particles. For $|K|>0$ high values of κ_h are associated with K, not the presence of small particles. Such errors are avoided if $M(H)$ is obtained to sufficiently high fields where significant departures from LSPM($1/H$, K=0) curves will be apparent, fig.7b. In environmental magnetism the presence of a significant high or moderate field susceptibility is often viewed as evidence of an independent 'paramagnetic' fraction and employed in source apportionment and fingerprinting. As high values of κ_h may be associated with K_u rather than a second phase this assumption should be treated cautiously. This is illustrated in fig.7a where sections of the $M(H)$ curves have been fitted employing three independent parameters, a, b and c to simulate LSPM and independent high field 'paramagnetic' phases, i.e., $M = aL(bB) + cB$ where $a = \varepsilon M_s$, $b = m/kT$, $c = \kappa_h/\mu_0$, $B = \mu_0 H$ and ε is the total particle volume fraction. This fitting procedure enables departure from pure Langevin dependence due to K and experimental curves to be readily characterised. Applied inappropriately, this method erroneously interprets the K dependent medium or high field linear variation in $M(H)$ as an independent paramagnetic term causing the particle volume parameter b, to be over-estimated ~70% and M_S, parameter a, underestimated by ~40%, table 1.

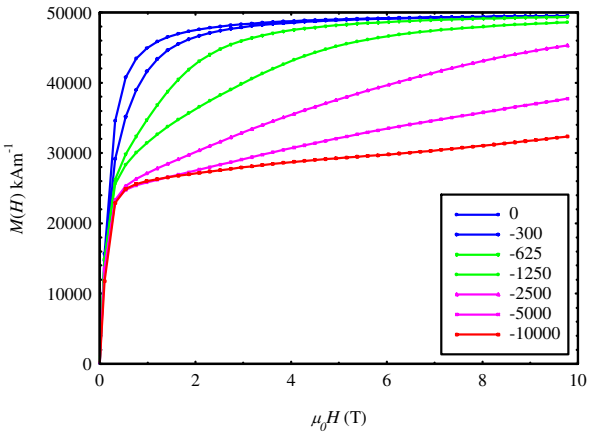

Fig.6a The effect of $K_u<0$ upon the SD $M(H)$ curve, b=10, ε=0.1

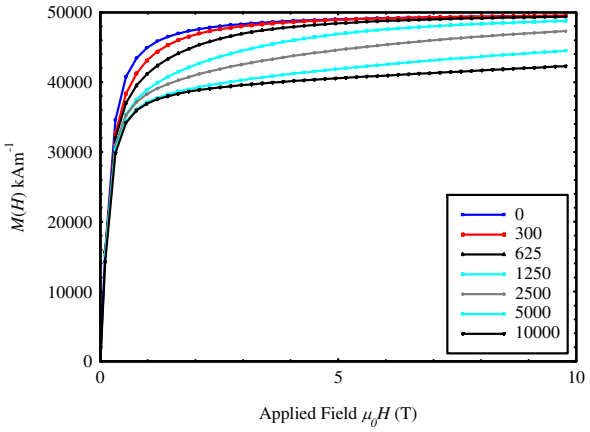

Fig.6b The effect of $K_u>0$ upon the SD $M(H)$ curve, b=10, ε=0.1

K (kJ m^{-3})	a (10^4)	b	c	Notes
0	5.0 (true a)	10 (true b)	0 (true c)	-
-300	3.43	13.1	10300	fit to 1T
-625	2.91	17.1	7500	fit to 2T
-1250	2.99	17.1	3600	fit to 3.5T
-2500	2.74	17.3	1980	fit to 10T
-5000	2.61	19.9	1230	fit to 10T
-10000	2.71	16.3	511	fit to 10T

Table 1 Result of employing fitting parameters a, b and c when $|K|>>0$.

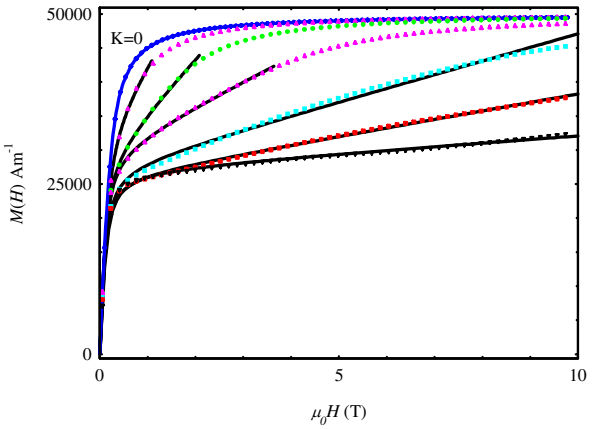

Fig.7a Use of three parameter fit to SD M(H) curves with negative anisotropy , computed for $M(b,K)$, b=10, K = 0, -300, -625, -1250, -2500, -5000, -10000 kJm^{-3}, see table 1

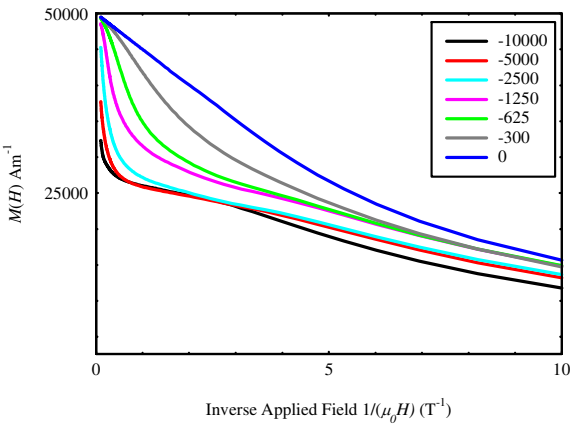

Fig.7b Use of $1/\mu_0 H$ to estimate M_s, for $M(b,K)$ of fig.7a

4. Concluding remarks - an analytical protocol

We suggest a protocol for the analysis of *M(H)* experimental data that seeks to minimise errors associated with the determination from experimental data of K, M_s, $\kappa(H)$, V and σ in SD systems:

1. Choose an appropriate pure magnetisation functional and attempt a single volume, (K=0) fit, parameter b determined from κ_i
2. Inspect $M(1/B)$ dependence
3. Employ a distribution function, κ_i dependent firstly upon b, secondly upon σ
4. Employ a single particle fit plus weak anisotropy
5. Combine 3 & 4
6. Employ high fields to separate K dependence from true high T paramagnetic component(s)
7. Inspect M/T superposition over temperature ranges sufficient to detect changes in K

5. References

[1] Weil L, 1954 *J. Chim. Phys*. **51** 715-717
[2] Neel L and Gruner L 1956 *Compt. Ren*d. **243** 1629
[3] Becker JJ 1957 *J. Metals, Trans. AIME* **209** 59
[4] Cahn J 1957, *J. Metals, Trans. AIME* Oct. **210** 1309
[5] Kilner M, Hoon SR, Lambrick DB, Potton JA and Tanner BK, 1984 *IEEE Trans Magn* **MAG 20** 1735, Hoon SR, Kilner M, Russell J and Tanner BK, 1983 *J. Mag. Magn. Matrls* **39** 107
[6] Chantrell RW Popplewell J and Charles SW, 1978 *IEEE Trans. Mag*. **MAG14** 975-977
[7] Chantrell RW Popplewell J and Charles SW, 1977 *Physica* **86-88B** 1421
[8] Tari A, Chantrell RW, Charles SW and Popplewell J, 1979, *Physica* **97B** 57, O'Grady K, Chantrell RW, Popplewell J and Charles SW,1980 IEEE Trans. Mag. **MAG16**, 1077
[9] Huber DL, Venturini EL, Martin JE, Provencio PR and Patel RJ, 2004 J. Mag. Magn. Matrls **278** 311
[10] Gaunt P 1968 Phil. Mag. **17** 263
[11] Franco V and Conde A, 2004 J. Mag. Magn. Matrls **277** 181, Franco V and Conde A, 2004 J. Mag. Magn. Matrls **278** 28
[12] Asimow RM, 1965 Trans Metall. Soc of AIME, **233** 401
[13] West FG, 1961 J. Appl. Phys. **32S** no3 249S